The Dynamics of Human Sperm Droplets on a Liquid Crystal and Polymer Composite Film

Farn Lu[1], Yi-Hsin Lin[2], Wan-Chen Tsai[1], Jiong-Juan Li[2], Ting-Yu Chu[2], Hsu-Kuan Hsu[3],

and Wang-Yang Li[3].

[1]Fertility Center, Ton Yen General Hospital,

No.69, Xianzheng 2nd Rd., Zhubei, Hsinchu, Taiwan, R. O. C.

[2]Department of Photonics, National Chiao Tung University,

1001 Ta Hsueh Rd., Hsinchu 30050, Taiwan, R.O.C

[3]Chi-Mei Optoelectronics Corp.,

No. 3, Sec. 1, Huanshi Rd., Tainan Science-based Industrial Park, Tainan , Taiwan, R. O. C.

ABSTRACT

A switchable surface using a liquid crystal and polymer composite film (LCPCF) based on phase separation between liquid crystals (LC) and polymers after photopolymerization is developed recently. The wettability of LCPCF is electrically tunable because of the orientation of liquid crystal directors anchored among the polymer grains under an in-planed electric field. A water droplet on the top of LCPCF can be manipulated under an inhomogeneous electric field on the LCPCF owning to the wettability gradient. The dynamics of a droplet of human sperms on the LCPCF is demonstrated as well. Three motions of sperm droplets are observed: the droplet collapse and the droplet stretch,. We found that the dynamics, concentrations, and activities of spermatozoa, affect the motions of a sperm droplet. The potential applications of LCPCF are polarizer-free displays, liquid lenses, and the microfluidic device in assisted reproductive technology (ART)

Keywords: liquid crystal, polymeric film, droplet manipulation,.biosensing

1. INTRODUCTION

Switchable surfaces based on self-assembled monolayers (SAMs) can switch wettability of surfaces by changing the conformation of molecules under external stimuli.[1-3] By properly controlling the distribution of wettability of the

Emerging Liquid Crystal Technologies V, edited by Liang-Chy Chien, Proc. of SPIE Vol. 7618,
761811 · © 2010 SPIE · CCC code: 0277-786X/10/$18 · doi: 10.1117/12.840680

switchable surfaces, a droplet on the surfaces can be driven toward the most wettable region because of the imbalance of the surface tension forces on the opposite sides of the droplet edge.[4-6] However, in the most of cases a drop of water refuses to move toward more hydrophilic region because the weak chemical gradient can not overcome the hysteresis. Many methods are published for manipulating droplets by obtaining gradient surfaces, such as thermal induced gradient,[7,8] vapor-phase diffusion,[9, 10] electrochemical method,[11] photoresponsive surface,[12] and photodegradation method.[13] Droplet manipulation has many applications, such as microfluidic devices, polarizer-free displays, and automobile windshields.[14, 15] Recently, we developed a different switchable surface, a liquid crystal and polymer composite film (LCPCF), by phase separation between liquid crystals (LC) and polymers after the photopolymerization.[16, 17] The wettability of LCPCF is electrically tunable because of the orientation of liquid crystal directors anchored among the polymer grains. In this paper, a droplet manipulation on LCPCF is demonstrated by an electrically controlled wettability gradient of LCPCF resulted from the spatially reorientation of liquid crystal molecules. The averaged translation velocity is around 1.17 mm/s. Furthermore, the LCPCF can be used to drive a sperm droplet for potential application of microfluidic devices. We also found the dynamics of spermatozoa affects the motion of semen droplet.

2. SAMPLE PREPARATION AND OPERATING PRINCIPLES

The structure of LCPCF and operating principles of a droplet manipulation of LCPCF are illustrated in Fig. 1(a) and (b). The structure consists of a LCPCF on a patterned ITO (indium tin oxide) glass substrate to provide in-plane electric fields. The ITO electrodes on the glass substrate were etched with interdigitated chevron patterns. The angle of the zigzag ITO stripes is 150^o. The width and gap of the electrode stripes are 4 μm and 14 μm, respectively. To fabricate the LCPCF,[16] we mixed a nematic LC mixture E7 (Merck) and a liquid crystalline monomer (4-(3-Acryloyloxypropyloxy)-benzoic acid 2-methyl-1, 4-phenylene ester) at 70:30 wt % ratios. The mixtures were then filled into an empty cell with a gap of 12 μm which consists of a glass substrate as a top substrate and a patterned ITO glass substrate as a bottom substrate. The top substrate of the cell was overcoated with a thin polyimide (PI) layer and then mechanically buffed at the direction of 20^o with respect to the electrode stripes. After filling, the cell was exposed to a UV light with intensity I = 10 mW/cm^2 for ~30 min at 70 °C. After phase separation and photo-polymerization, the top glass substrate was peeled off by a thermal releases process. A solidified LCPCF was obtained with 12 μm thickness and 30 nm root-mean-squared roughness, as depicted in Fig. 1(a). The magnification of the LCPCF surface including polymer grains and liquid crystals among polymer grains in Fig. 1(a) is exaggeratedly illustrated in Fig. 1(b). At V=0, the LC directors are aligned along y-direction, parallel to the rubbing direction of the PI layer. Under an applied AC voltage (f = 1 kHz), LC directors are reoriented along the electric fields. The LCPCF is more hydrophobic at 0 V_{rms} because the phenyl planes of LC molecules are more parallel to the surface of the LCPCF (x-y plane). On the contrary, the LCPCF is more hydrophilic at high AC voltage because of the field-induced uneven tilts of the terminal groups of LC molecules near the edges of the fringe electric fields on the LCPCF surface. Moreover, the hydrophile of the LCPCF is electrically tunable by changing the magnitude of the AC voltage. In order to manipulate a droplet, the two regions of the interdigitated chevron electrodes were patterned identically, as shown in Figs. 2(b), 2(c), and 2(d) . The droplet on LCPCF can be driven by an imbalanced Young's force,[5,9] which arises from wettability gradient of LCPCF induced by orientation of LC molecules under a periodically applied inhomogeneous electric field, as shown in Fig. 2(a). The contact angles on both sides of the droplet are the same at V=0. The contact angle on the left is smaller when we apply AC electric field in the left region of electrodes because the left region of LCPCF is more hydrophilic. The droplet is then driven toward more hydrophilic region.

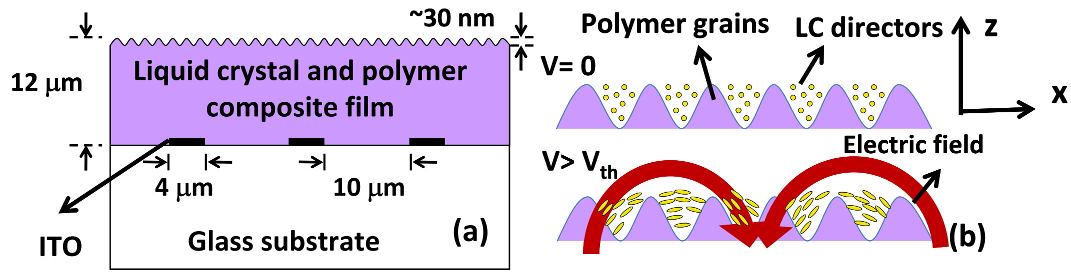

Fig. 1. (a)Schematic structure and (b) operating principles of LCPCF.

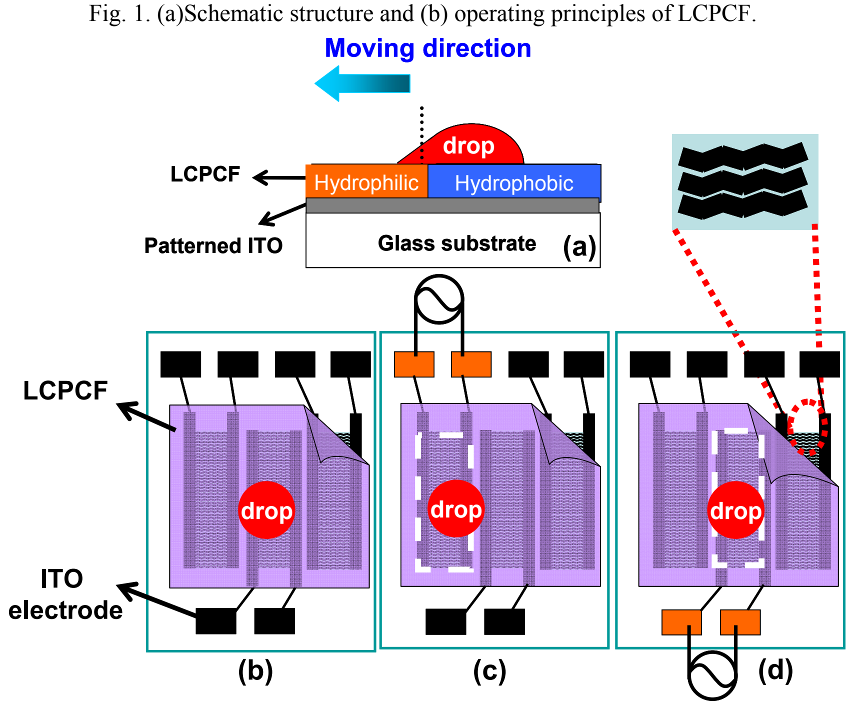

Fig.2. (a)Schematic droplet manipulation on wettability controllable LCPCF in side view. The droplet manipulation on LCPCF in top view when (b)the voltage is off, (c)the voltage is applied on the left electrode region, and (d) the voltage is applied on the middle electrode region.

3. EXPERIMENTAL RESULTS

Fig. 3 shows the image of scanning emission microscopy of the surface of LCPCF after we removed the LC by hexane. The surface also shows elongated aggregation of polymer grains along the rubbing direction and void holes for LC molecules. The LCPCF surface replicates the rubbing patterns after peeling off the top glass substrate which was coated with a polyimide layer. The size of LC domains is around 100-200 nm. The root-mean-square (RMS) roughness of the film surfaces was measured to be ~30 nm by an atomic force microscope (AFM) (Dimension 3100, Digital Instruments) at tapping mode at the room temperature (~23^{o}C) in air.

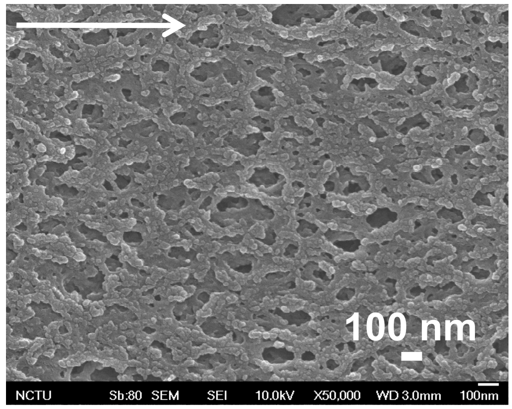

Fig. 3 The SEM image of LCPCF. The arrow indicates the rubbing direction before peeling off the top substrate.

To observe a droplet movement on the LCPCF under inhomogeneous in-plane electric fields, we recorded the dynamics of the droplet and measured contact angles of the droplet with time. A 3 μl drop of the de-ionized water was deposited on the LCPCF. We applied 250 V_{rms} squared pulses (f = 1 kHz) to the left region of electrodes only for the time duration of 600 ms. Figure 4 (a) and (b) show the measured results. In Fig. 4(a), the droplet moved like a caterpillar with time when we applied a periodic electric field in the left region of electrodes. The reason why we used periodically electric fields is mainly to overcome the hysteresis of the surface and then make the droplet moved forward. The translation distance of the center of mass of the droplet is around 0.7 mm in 0.6 sec. As a result, the averaged velocity is around 1.17 mm/sec. The droplet stops till the center of mass of the droplet is in the middle of two electrode regions. The water contact angle as a function of time is shown in Fig. 4(b). We did measurements 6 times and averaged the results. The water contact angle changes periodically with applied electric fields. The water contact angle on the left is smaller than the one on the right because the left region of LCPCF is more hydrophilic resulting from the orientation of LC molecules. When we turned on the voltage at 0.9 sec, the contact angle difference between left (~61^o) and right (~73^o) of the droplet was around 12^o. The droplet started to accelerate and then slowed down with the reduction of the contact angle difference between the left and the right contact angles. The droplet tends to be in more hydrophilic region and then moves from the right to the left.

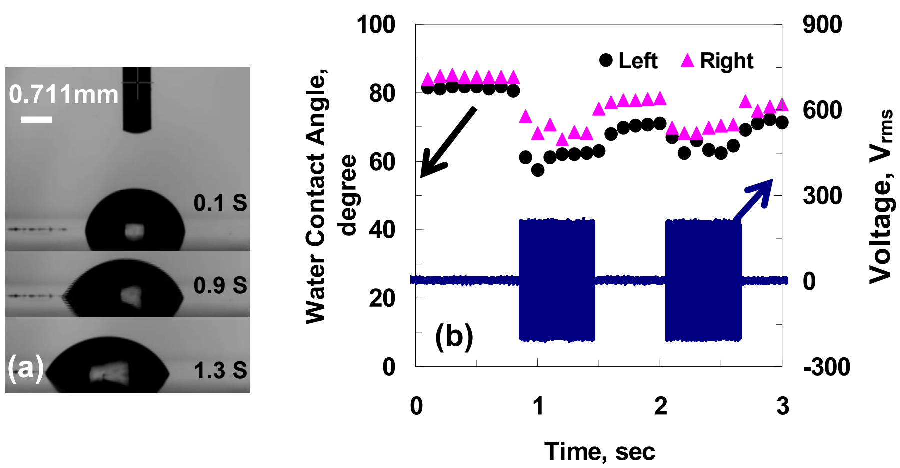

Fig. 4. (a) The photos of water droplet manipulation at 0.1, 0.9 and 1.3 sec. (b) The water contact angle as a function of time under a squared pulsed voltage (250 V_{rms}) with 600 ms time duration

The droplet moves when the contact angle on the right is greater than the angle on the left. As a result, the Laplace pressure is greater at right edge than at the left edge. The droplet motion occurs from a higher to a lower pressure; thus, the droplet moves from the right to the left. The driving force of the droplet per unit length (F_d) can be expressed by the variation of surface energy (U) in a small distance (dx).[5]

$$dU = -F_d \cdot dx \tag{1}$$

where dU can be expressed as the surface tension difference between the left and the right of the droplet:

$$dU = [(\gamma_{SL} - \gamma_{SV})_{left} - (\gamma_{SL} - \gamma_{SV})_{right}] \cdot dx \tag{2}$$

where γ represents the surface tension (i.e., energy per unit surface) of the interface, and S, L, and V indicate the phases of the solid, liquid and vapor. From Eqs. (1) and (2), the driving force per unit length is

$$F_d = -(\gamma_{SL} - \gamma_{SV})_{left} + (\gamma_{SL} - \gamma_{SV})_{right} \tag{3}$$

Assumed that θ_{right} and θ_{left} stand for the local contact angles on the right and on the left of the droplet which satisfy Young's equation, Eqn. (3) can be represented as

$$F_d = \gamma_{LV}(\cos(\theta_{right}) - \cos(\theta_{left})) \tag{4}$$

The contact angle is larger on left than on right. Therefore, the droplet moves towards left. We can adjust the electric fields to reorient LC molecules and further control the distribution of spatial wettability of the LCPCF. As a result, the motion of a droplet can then be manipulated. The droplet movement also depends on the viscous resistance force resulting from the interface between liquid and solid.

To observe the motion of a semen droplet on LCPCF, we replaced water droplets by the semen samples donated by 34 males between 26 and 45 years old. The image of semen is shown in Fig. 5. We did the same experiment for manipulating a semen droplet of 1.5 μL. Instead of droplet translation, two motions of semen droplets were observed: collapse and back-and-forth stretch. Here, collapse of a droplet means the contact angle changes immediately when we turn on the voltage and then the contact angle does not recover when we turn off the voltage. And back-and-forth stretch of a droplet means the contact angles of a droplet changes periodically with pulsed voltages, but the droplet stay in the same location. Semen droplets cannot do the translation motion because of their high viscosity. As a result, the imbalanced force of the semen droplet can not move the semen droplet forward. We observed the motion of semen droplet on LCPCF and compared the parameters of standard semen analysis, such as concentration, motility which is the ratio of motile spermatozoa (or sperm) to total sperm number, grade I defined as the percentage of spermatozoa moving in circles, grade II defined as the percentage of spermatozoa swimming in a forward direction, and morphology which indicates the percentage of normal sperm heads. According to World Health Organization (WHO) guidelines, a standard sperm analysis is performed for measuring the parameters of spermatozoa.[18, 19] The concentration, motility, grade I, and grade II were counted by Makler counting chamber (Irvine Scientific). Spermac stain method (sps250, FertiPro) was used for assessing sperm morphology. Table 1 is listed the results of the motility, morphology, grade I, and grade II, semen concentration for the collapse and the stretch of semen droplets. The droplet stretches back and forth only when the semen concentration is larger than 100 million/mL, morphology is larger than 15 %, motility is larger than 50%, grade I is less than 30%, and grade II is larger than 30%. Otherwise, the semen droplet collapses. A man with semen of higher concentration, and higher motility, will have a better chance to get conception. The low grade I and high grade II of semen which means more motile spermatozoa that move in a straight line with good speed are preferred to natural conception. The high morphology of semen which means fewer abnormal spermatozoa can lower the likelihood of infertility. Therefore, the stretch or collapse of a semen drop serves the purpose of probing the quality of spermatozoa. The stretch of a semen drop shows the better quality of semen than the collapsing one for human reproduction. The reason why sperm droplet stretch is because seminal plasma flows which is induced by wettability gradient. The weak or immobile spermatozoa are brought by the flow of semen plasma; however, the motile and strong enough spermatozoa swim against the flow of semen plasma. As a result, spermatozoa that swim opposite to the flow direction drag the semen drop back. Therefore, the semen droplet stretches back and forth with applied pulsed voltage in the left region. The high concentration, high motility, better morphology, low grade I, and high grade II representing more spermatozoa can swim upstream against the flow current of seminal plasma induced by the wettability gradient of LCPCF. The semen droplet collapse is not only because of flush of the seminal plasma induced by the wettability gradient, but also because of the attraction and traps of weak or immobile spermatozoa by the field of liquid crystals and weak fringing electric fields on the surface of LCPCF. The surface of LCPCF is then re-modified. Therefore, the switchable properties of LCPCF are invalid by the cover of the spermatozoa.

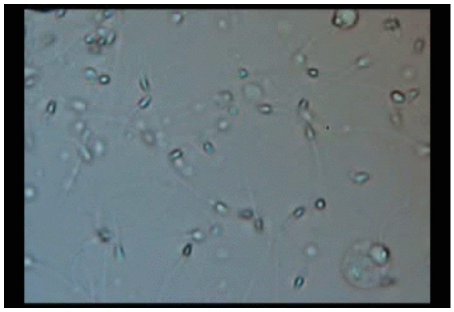

Fig. 5. (a)The image of sperms.

Semen drop	Stretch	Collapse
Concentration, M/mL	>100	<100
Motility, %	>50	<50
Morphology,%	>15	<15
Grade I, %	<30	>30
Grade II, %	>30	<30

Table 1 The stretch and collapse of sperm droplets depend on sperm parameters.

4. CONCLUSION

In conclusion, we demonstrated the motions of a semen droplet on a switchable LCPCF surface. The better quality of spermatozoa results in back-and-forth stretches of a semen drop on LCPCF; otherwise, collapse of semen drops. In fact, fertilization is involved many complicated sperm-oocyte process, not decided by sperm quality only. However, good sperm quality is still a significant factor for fertility potential. Here, the experimental results indicate the great potential of LCPCF for a sperm tester of sperm quality. Other potential applications of LCPCFs are polarizer-free displays, liquid lenses, and the microfluidic device in assisted reproductive technology.

Acknowledgments

The authors are indebted to Ms. Liang-Chieh Peng, Ms. Pi-Yu Chen (Ton Yen General Hospital), Prof. Shu-Hsia Chen (NCTU), Mr. Wei-Lin Chu (NCTU), and Dr. Yung-Hsun Wu (Innolux Display Corp.) for useful discussions and technical assistance. This research was supported by National Science Council (NSC) in Taiwan under the contract No. 98-2112-M-009-017-MY3.

REFERENCES

[1] J. Lahann, S. Mitragotri, T. Tran, H. Kaido, J. Sundaram, I. S. Choi, S. Hoffer, G. A. Somorjai, and R. Langer, Science **299,** 371 (2003).

[2] Liu, L. Mu, B. Liu, and J. Kong, Chem. Euro. J. **11,** 2622 (2005).

[3] S. L. Gras, T. Mahmud, G. Rosengarten, A. Mitchell,and K. Kalantar-zadeh, Chemphyschem **8**, 2036 (2007).

[4] P. G. de Gennes, Rev. Mod. Phys. **57,** 827 (1985).

[5] P. De Gennes, F. Brochard-Wyart, and D. Quere, *Capillarity and Wetting Phenomena Drops, Bubbles, Pearls, Waves* (Springer-Verlag, Berlin, 2004)

[6] H. Bruus, *Theoretical Microfluidics* (Oxford University Press, New York, 2008)

[7] F. Brochard, Langmuir **5**, 432 (1989)

[8] A. M. Cazabat, F. Heslot, S. M. Troian, P. Charles, Nature **346**, 824 (1990)

[9] M. K. Chaudhury, and G. M. Whitesides, Science **256** 1539 (1992)

[10] S. Daniel, and M. K. Chaudhury, Langmuir **18** 3404 (2002)

[11] B. S. Gallardo, V. K. Gupta, F. D. Eagerton, L. I. Jong, V. S. Craig, R. R. Shah, and N. L. Abbott, Science **283**, 57 (1999)

[12] K. Ichimura, S. K. Oh, and M. Nakagawa, Science **288** 1624 (2000)

[13] Y. Ito, M. Heydari, A. Hashimoto, T. Konno, A. Hirasawa, S. Hori, K. Kurita, and A. Nakajima, Langmuir **23** 1845 (2007)

[14] P. Tabeling, *Introduction to Microfluidics* (Oxford University Press, New York, 2005)

[15] R. A. Hayes, and B. J. Feenstra, Nature **425** 383 (2003)

[16] Y. H. Lin, H. Ren, Y. H. Wu, S. T. Wu, Y. Zhao, J. Fang, and H. C. Lin, Opt. Express **16** 17591 (2008)

[17] H. Ren, S. H. Wu, and Y. H. Lin, Phys, Rev. Lett. **100** 117801 (2008)

[18] World Health Organization. *WHO Laboratory Manual for the Examination of Human Semen and Sperm-Cervical Mucus Interaction 4th edition* (Cambridge University Press, 1999)

[19] Jeyendran, R. *Protocols for Semen Analysis in Clinical Diagnosis* (Parthenon Publishing Group, 2003)